ACS APPLIED MATERIALS & INTERFACES

Research Article

www.acsami.org

Elastic Stiffness and Filler Size Effect of Covalently Grafted Nanosilica Polyimide Composites: Molecular Dynamics Study

Seunghwa Yang, Joonmyung Choi, and Maenghyo Cho*

Division of WCU Multiscale Mechanical Design, School of Mechanical and Aerospace Engineering, Seoul National University 599, Kwanak-Ro, Kwanak-Ku, Seoul151-744, Korea

ABSTRACT: The filler size-dependent elastic stiffness of nanosilica (α-quartz)-reinforced polyimide(s-BPDA/1,3,4-APB) composites under the same volume fraction and grafting ratio conditions was investigated via molecular dynamics(MD) simulations. To enhance the interfacial load transfer efficiency, we treated the surface oxygen atoms of the silica nanoparticle with additional silicon atoms attached by a propyl group to which the aromatic hydrocarbon in the polyimide is directly grafted. As the radius of the embedded nanoparticle increases, the Young's and shear moduli gradually decrease, showing a prominent filler size effect. At the same time, the moduli of the nanocomposites increase as the grafting ratio increases. The contribution of different nanoparticles to the filler size dependency in elastic stiffness of the nanocomposites can be elucidated by comparing the normalized adhesive interaction energy between the particle and matrix which exhibits prominent filler size dependency. Because of the immobilization of the matrix polymer in the vicinity of the nanoparticles, which was confirmed by the self-diffusion coefficient, the highly grafted interface is found to bring about a greater reinforcing effect than the ungrafted interface.

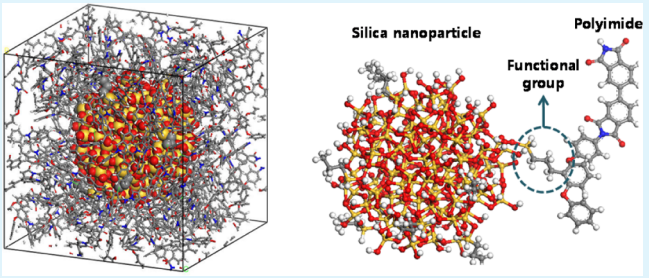

KEYWORDS: *nanocomposites, covalent grafting, size effect, molecular dynamics, nanosilica, polyimide*

INTRODUCTION

With the rapid advancement of the manufacturing techniques for nanostructured materials, polymer nanocomposites that contain nanosized fillers have received considerable attention.[1−5] Behind the potential applicability of nanocomposites are their expected multifunctionality and the onset of unusual properties that originate from the structural ordering and densification of the matrix polymer in the vicinity of the nano fillers. As the ratio of the surface area to volume increases on the nanometer scale, more of the surface atoms in the nanofillers can interact with more of the matrix molecules, especially in the interphase zone. From a geometrical point of view, under the assumption that the thickness of the densified interphase near the nanofiller is constant, the relative volume fraction of the interphase increases as the size of the nanofiller decreases.[6] Thus, the interfacial strength and molecular adsorption to the surface of the nanofiller which develops an interphase is the key to the filler size-dependent overall properties of the nanocomposites.

Regarding the mechanical properties, Cho et al.[7] compared the reinforcing effect of nanosized alumina (Al_2O_3) particles with their micrometer-sized counterparts embedded into a vinyl ester matrix. In the nano alumina reinforced composites, the resultant elastic modulus and tensile strength increased as the size of the alumina decreased, while no obvious trend was observed from the micrometer-sized alumina embedded specimens at 1 vol% loading. Chisholm et al.[8] demonstrated a similar tendency of the filler size dependent elastic moduli of epoxy-based silicon carbide(SiC) composites by comparing the nano SiC and micrometer SiC embedded specimens. Studies on nano calcium carbonate($CaCO_3$) particle reinforced polypropylene composites,[9] nano titanium dioxide(TiO_2) embedded epoxy composites,[10] and nanosilica reinforced polysiloxane coatings[11] showed the same filler size-dependent tensile properties, thus demonstrating the excellence of such nanocomposites. Besides the tensile properties, the thermal stability and coefficient of thermal expansion(CTE) can also be tuned by using nano fillers.[12,13]

From molecular dynamics(MD) simulations, the size effect of nanocomposites and the detailed structural analysis of the interphase molecules near the particles have been intensively studied to develop structure−property relationships. For its chemical rigorousness and usefulness in describing behaviors of condensed matters, the MD simulation has been widely used to predict the properties of polymeric materials and local interaction problem of material interfaces.[14−16] Adnan et al.[17] considered different types of buckyball as nanoparticles embedded into a polyethylene matrix. Not only the overall elastic properties of the nanocomposites, but also the magnitude of the densification of the matrix polymer close to the buckyball, have been found to be clearly dependent on the size of the nanoparticles. Yang and Cho,[18,19] Yu et al.,[20] and Liu

Received: June 24, 2012
Accepted: August 29, 2012
Published: August 29, 2012

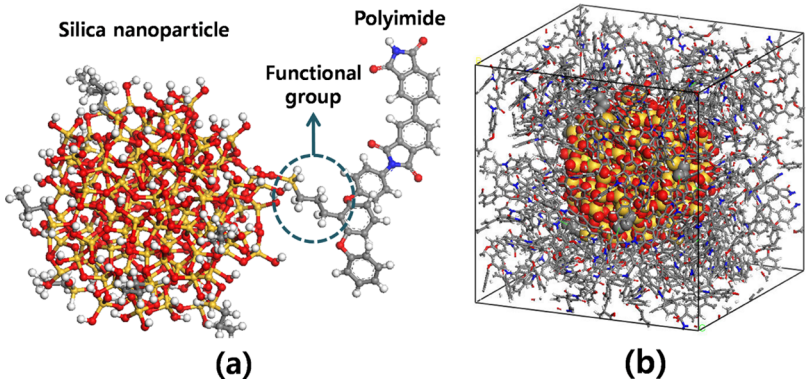

Figure 1. Molecular model of covalently grafted nanocomposites. (a) Surface-treated silica nanoparticle and covalent grafting via a functional propyl group to the aromatic carbon atom of the polyimide (b) Covalently grafted silica/polyimide nanocomposites periodic unit cell after finishing the covalent grafting process according to the predefined grafting ratio.

et al.[21] found the same tendency wherein the smaller nanoparticles are more appropriate to increase the elastic stiffness of the composites by performing MD simulations on nanoparticulate polymer nanocomposites. They traced the radial density profile of the surrounding matrix polymer and indentified a clear peak that indicates the formation of an interphase. Moreover, from MD simulations[22] and Monte Carlo simulations,[23] it was found that the local stress and modulus distribution of the matrix molecules have a clear spike near the nanofiller and gradually converge to the values of the bulk matrix. More recently, the effect of the filler size on the thermal expansion coefficient of SiC/epoxy nanocomposites was reported.[24,25] In these atomistic simulation results, the filler size-dependent properties have been correlated with the condensation of the surrounding matrix molecules, which has been experimentally revealed by several different measurements and strategies.[26−29]

To improve the interfacial strength and increase the proportion of confined interphase, researchers have used various types of covalent and noncovalent grafting in the manufacture of nanocomposites.[30−35] The two main purposes of these treatments are to enhance the dispersion of the fillers and to strengthen the interaction between the filler and matrix to achieve better performance of the designed nanocomposites.[35,36] Covalent grafting, in particular, is a promising way to increase the load transfer efficiency by taking advantage of the strong interatomic force of the covalent bonds by inducing the interpenetration of the free and grafted chains in the vicinity of the nanofillers. Referring to the work by Ndoro et al.[37] on the molecular level structural analysis of grafted nanocomposites, increasing(decreasing) the radius(curvature) of the nanoparticles inhibits the penetration of the free chains near the nanoparticles, which can cause the load transfer efficiency to be reduced. At the same time, they also pointed out that the interpenetration is more disturbed as the grafting density increases.

Herein, we consider the filler size dependency of the overall elastic moduli of covalently grafted nanosilica reinforced polyimide composites via MD simulations. Under the same volume fraction conditions, the variation of the elastic moduli of the nanocomposites with the radius of the embedded particles is investigated, in order to provide a practically meaningful reference for the filler size effect. The effect of the number of covalently bonded sites on the overall landscape of the filler size dependent variation of the elastic moduli is investigated by considering two different grafting ratios and by comparing the resultant elastic moduli with those of the ungrafted nanocomposites.[19]

MOLECULAR MODELING AND SIMULATION PROCEDURES

In all molecular modeling and simulation procedures, a commercially available MD simulation package Material Studio 5.0 (Accelrys Inc., San Diego, CA)[38] with the COMPASS force field for inter- and intra-atomic interactions was used.

The silica nanoparticles were trimmed from bulk α-quartz in the form of spherical inclusions. In this study, we considered eight different nanoparticles having different radii ranging from 9.97 Å to 13.97 Å. In the spherical nanosilica, all of the free radicals of the silicon atoms are first treated by oxygen atoms to mimic the real oxidation process. Then, candidates of the covalent grafting are randomly chosen from all of the surface oxygen atoms that have one free radical. Once the surface oxygen atom is chosen as the nominee for further processing to make a direct covalent bond with the matrix molecules, it is again treated with a silicon atom which is attached by a propyl group. The end carbon of the propyl unit then acts as a linker atom to be covalently bonded to the aromatic hydrocarbon of the matrix molecules, as shown in Figure 1a. The functional units were attached to the surface oxygen atoms in the nanoparticles before the nanoparticle is embedded into the nanocomposites periodic unit cell.

To identify the effect of the covalent grafting ratio, we considered two different grafting ratios of 5 and 10% and the number of grafting sites according to the radius of the nanoparticle and the grafting ratio are shown in Table 1. Here, the grafting density is defined as the number of grafted functional units per unit surface area of the nanoparticles. Even at the same grafting ratio, the number of grafted

Table 1. Nanoparticles and Number of Grafting Sites for Nanocomposites System

			no. of grafting sites		grafting density(units/nm^2)	
case	particle radius (Å)	no. of surface oxygen atoms	5%	10%	5%	10%
1	9.97	104	5	10	0.40	0.80
2	10.74	104	5	10	0.34	0.69
3	11.41	128	6	12	0.36	0.73
4	12.01	140	7	14	0.38	0.77
5	12.56	148	7	14	0.35	0.70
6	13.06	160	8	16	0.37	0.74
7	13.53	180	9	18	0.39	0.78
8	13.97	192	10	19	0.40	0.77

dx.doi.org/10.1021/am301144z | ACS Appl. Mater. Interfaces 2012, 4, 4792−4799

sites increases as the radius of the nanoparticle increases, whereas the grafting density fluctuates according to the radius of the nanoparticle without showing any increasing or decreasing trends.

During the covalent grafting generation process, we assumed that only the hydrocarbon atoms in the aromatic ring of the polyimide can make covalent bonds with the linker atom in the nanoparticle. Each polyimide chain considered is composed of a total of ten unit monomers of s-BPDA/1,3,4-APB which has ever been considered in molecular dynamics simulation on the silica nanocomposites.[18,19,39,40] We fixed the volume fraction of the nanocomposites at 12% so that the particle radius would be the only variable to be correlated with their overall performance of nanocomposites at each grafting ratio.

After the individual molecular structures of the surface-treated silica nanoparticle and polyimide chains are prepared, the periodic unit cells of the nanocomposites, in which the silica nanoparticle is embedded at the center, are constructed using the Amorphous cell module of Material Studio 5.0. The final target density for the construction of the unit cell of the nanocomposites was set to 1.3 g/cm^3. As the polyimide molecules have aromatic rings, ring spearing and catenation resulting in the unrealistic behavior of the polymer molecules may occur during the cell construction process. Thus, the cell construction starts with a small target density of 0.1 g/cm^3 followed by 1000 steps of potential energy minimization via the conjugate gradient method and 1000 steps of isothermal ensemble, often referred to as NVT ensemble simulation[41] with rigorous checking for the spearing and catenation of the ring. Then, the target density increases in turn and the same energy minimization and ensemble simulation are followed until the final target density of the unit cell is reached. The compositions of the unit cells of the periodic nanocomposites RVE (representative volume element) are listed in Table 2.

Table 2. Unit Cell Composition of Nanocomposites

			cell length (Å)		volume fraction	
case	particle radius (Å)	no. of polyimide molecules	5% grafted	10% grafted	5% grafted	10% grafted
1	9.97	4	33.01	32.98	0.115	0.115
2	10.74	5	35.05	35.38	0.120	0.117
3	11.41	6	38.33	37.65	0.119	0.116
4	12.01	7	39.53	39.86	0.117	0.114
5	12.56	8	41.28	41.27	0.118	0.118
6	13.06	9	42.70	42.83	0.119	0.118
7	13.53	10	44.35	44.52	0.119	0.117
8	13.97	11	45.84	46.03	0.118	0.117

After the initial periodic unit cells are prepared, the covalent grafting process is performed. In order to search for the candidate for covalent grafting, all of the close contacts between the linker carbon atom in the nanoparticle and the hydrocarbon in the polyimide are monitored and the closest contact is detected. If the closest contact is within a predefined cutoff radius, then a new bond is formed and the potential energy of the whole structure is minimized using the updated potential parameters according to the newly bonded structure. Otherwise, a larger cutoff distance is defined and the same close contact detection procedure is performed. The default cutoff radius in the grafting process was set to 4 Å and the maximum cutoff radius to complete the covalent grafting was set to 6 Å. We again checked for ring spearing right after the formation of the covalent bond between the nanoparticle and matrix. The basic idea for the covalent grafting process used in the present simulation is quite similar to that of the cross-linking process used for the modeling of thermoset epoxy molecular structures.[42]

After finishing the covalent grafting process, 100 ps of isothermal–isobaric ensemble referred to as NPT ensemble simulation[41,43] at 600 K and 1 atm with a time integration step of 1 fs was followed. Finally, all of the unit cells were again equilibrated at 300 K and 1 atm through 1.3 ns of NPT ensemble simulations. During the final equilibration process, all of the position, momentum, and thermodynamic properties were stored every 1000 steps for post processing. The cell size and resultant volume fraction of the nanocomposites are shown in Table 2. After the 1.3 ns of equilibration, the volume fraction of each nanocomposite is almost 12% and, thus, the unit-cell equilibration process is successful.

As a final production run, a Parrinello-Rahman's constant stress ensemble simulation expressed as NσT[44] was applied to use Parrinello-Rahman's fluctuation method[45] to calculate the elastic stiffness tensor given as

$$C_{ijkl} = \frac{kT}{\langle V \rangle} \langle \delta\varepsilon_{ij} \delta\varepsilon_{kl} \rangle^{-1} \quad (1)$$

where C_{ijkl}, V, and ε_{ij} are the stiffness tensor, volume, and strain of the unit cell, respectively, and k is the Boltzmann constant. The brackets $\langle \bullet \rangle$ indicate the ensemble average. In the $N\sigma T$ ensemble, we set the magnitude of the stress tensor as −1 atm, which is equivalent to the atmospheric pressure, thus, the elastic stiffness obtained from eq 1 is at atmospheric pressure. The $N\sigma T$ ensemble simulation was performed for 600 ps to gather the strain fluctuations and other quantities required for the strain fluctuation method. At this stage, we only considered the strain fluctuation stored during the final 100 ps of the simulation, while the previous 500 ps of the simulation was assigned as the final equilibration process at 300K and 1 atm. In applying eq 1 to calculate the elastic stiffness, a total of 10 000 strain fluctuations were stored and considered. For the sake of the computational accuracy, we repeated the final strain collection simulation five times and the elastic stiffness tensor was averaged over the five different stiffness tensors.

RESULTS AND DISCUSSION

Elastic Moduli of Nanocomposites. The Young's and shear moduli of the 5 and 10% grafted nanocomposites obtained from the strain fluctuation are depicted in Figure 2 with their standard deviations and compared with the results for the ungrafted nanocomposites reported in a previous work on the same silica/polyimide nanocomposites.[19] As a reference

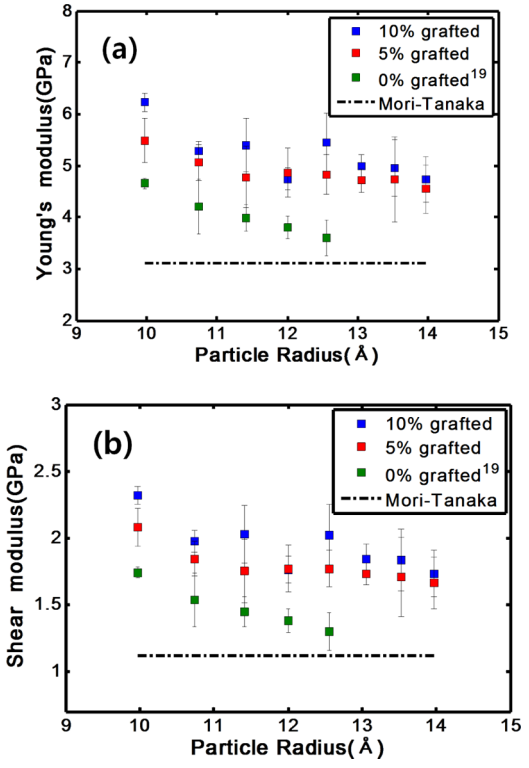

Figure 2. Elastic moduli of nanocomposites obtained from the MD simulations: (a) Young's moduli, (b) Shear moduli.

to highlight the particle size effect, a conventional micromechanics model prediction via the Mori-Tanaka model is attached. As shown in the previous study on the ungrafted nanocomposites,[19] both the Young's and shear moduli increase as the radius of the nanoparticle decreases. At the same time, by increasing the grafting ratio from 0% to 10%, the elastic constants of the nanocomposites increase as expected. The enhancement of the elastic constants is clearer in the range from 0 to 5%, whereas it is less distinguishable in the range from 5% to 10%. Even if a grafting ratio larger than 10% had not been considered, we conjecture that there is a limiting point in the grafting ratio at which the enhancement of the elastic moduli of the nanocomposites becomes insignificant.

Compared with the variation of both moduli in the case of a grafting ratio of 0%, the variations of the moduli in the case of the grafted nanocomposites are more gradual and have long-range transitions. Thus, the particle size effect is expected to be valid even for larger nanoparticles by addressing the covalent grafting. However, the range of the particle size effect in the case of the ungrafted nanocomposites is narrow and seems to converge to a particle diameter of 3 nm. Considering the typical ranges of the embedded particle size effect even above a particle diameter of 10−20 nm that have been observed in real experimental measurements, such a small range seems disappointing, however, most of the manufacturing processes used for nanocomposites adopt special surface treatment and covalent grafting, such as in situ polymerization, to enhance the interfacial strength. From this point of view, the present molecular dynamics simulation results reflect a more realistic evolution of the particle size effect than the previous results with pristine nanoparticles. For the present simulation results, it is expected that the particle size effect can manifest itself even at a particle diameter of 10 nm, which is quantitatively closer to the experimentally observed size effect. To achieve a more reasonable estimation of the range of the size effect at various volume fractions, additional MD simulations on larger nanoparticle embedded nanocomposites unit cells are required in order to obtain the overall contour of the elastic moduli. However, the computational cost for such simulations would be enormous. Instead, the application of continuum-based analytical solutions to predict the effective elastic moduli of the nanocomposites can be alternatively utilized to save the computation time without reducing the accuracy to capture the size effect.[19] In the near future, a multiscale modeling approach considering the grafting ratio and the size effect in a constitutive model will be developed as an extension of the present study.

The radius of gyration (R_g) of the polyimide matrix surrounding the silica nanoparticle before generating the covalent grafting is shown in Table 3. In general, it is known that the embedded filler size effect is highly related to the radius of gyration of the matrix polymer. Regardless of the radius of the silica nanoparticle, the radius of gyration of the surrounding polymer is about 13 Å, which is quite close to the particle radius to which the size effect in elastic moduli of 0% grafted nanocomposites converges. At a finite percentage of covalent grafting, however, the possible range of the particle size effect is much larger than the radius of gyration of the ungrafted polymer. Even though we did not further investigate the correlation between the radius of gyration of the matrix polymer and the properties of grafted nanocomposites, it can be reasonably concluded that the radius of gyration shown in Table 3 can be a useful indicator to predict the critical diameter of the nanoparticle below which the particle size dependent properties of the ungrafted nanocomposites appear.

Table 3. Radius of Gyration of Polyimide Molecules in Nanocomposites before Grafting

particle radius (Å)	no. of polyimide molecules	radius of gyration, R_g(Å)	std. deviation (Å)
9.97	4	12.19	0.39
10.74	5	13.53	0.91
11.41	6	13.99	2.05
12.01	7	13.10	1.39
12.56	8	11.84	0.98
13.06	9	12.98	0.58
13.53	10	13.09	1.00
13.97	11	12.55	0.9

Interaction Energy between Nanoparticle and Polymer Matrix. Compared with the conventional continuum model prediction shown in Figure 2, there are three unusual characteristics of the nanocomposites, especially in the case of the grafted ones; the filler size effect, stiffening by the covalent grafting, and the variation of the elastic moduli according to the particle radius. In order to elucidate these characteristics in terms of the nonbonding interaction between the particle and matrix and the local diffusivity of the polyimide matrix molecules, a single point interaction energy between the nanoparticle and matrix at the end of the equilibration simulation at 300 K and 1 atm, as well as the mean squared displacement (MSD) of the polyimide matrix during the last 300 ps of the same equilibration simulations, are investigated.

The nonbonding interaction energy between the silica nanoparticle and polyimide matrix at the end of the equilibration process can be obtained as

$$U_{\text{interaction}} = U_{\text{comp}} - U_{\text{mat}} - U_{\text{par}} \quad (2)$$

where the subscripts "comp", "mat", and "par" indicate the nanocomposites, matrix phase molecules, and nanoparticle, respectively. As the radius of the embedded nanoparticle in the nanocomposites increases, the number of atoms in the surrounding polyimide consequently increases and, thus, a larger nanoparticle in the nanocomposites can have a greater number of nonbonding pairs. Apparently, the neat nonbonding interaction energy between the nanoparticle and surrounding matrix increases as the size of the embedded nanoparticle increases. However, for the qualitative correlation of the interaction energy with the resultant elastic moduli of the nanocomosites which is an intensive property, the interaction energy should be converted to an intensive property as well. Thus, the interaction energies between the nanoparticle and matrix, which is normalized by the volume of the nanoparticles, are compared with each other and depicted in Figure 3. The interaction energies between the silica nanoparticle and polyimide are adhesive in nature and their magnitude decreases as the size of the nanoparticle increases. As the size of the embedded nanoparticle increases, a greater proportion of the atoms in the nanoparticle are located at the surface and, thus, the number of nonbonding pairs between the nanoparticle and matrix increases. However, the surface to volume ratio of the nanoparticle decreases as the size of the nanoparticle increases, thus, the number of nonbonding pairs per unit volume of the nanopartice decreases. This is the reason why the magnitude of the normalized interaction energy in Figure 3 decreases according to the radius of nanoparticle. In this respect, the ideal structure that can maximize the size effect is a hollow one,

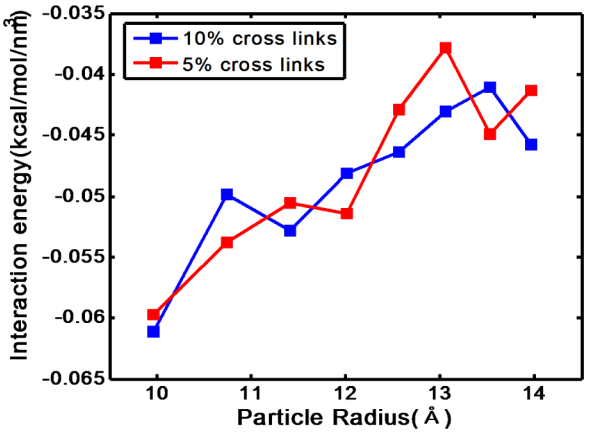

Figure 3. Nonbond interaction energy between the silica nanoparticle and polyimide matrix normalized by the volume of the embedded nanoparticle.

such as nanotubes or buckyballs, where all of the atoms are located only at the surface. At the same time, the polymer densification in the vicinity of the nanoparticle plays an important role in showing the particle size effect, not only energetically, but also structurally. Energetically, since the number density of the interphase zone is higher than that of the pure base polymer, the number of nonbonding interaction pairs between the nanoparticle and matrix is increased compared with the situation where the nanoparticle is surrounded by the bulk polymer having a smaller density than the interphase zone. Structurally, the densification of the polymer molecules naturally leads to a local hydrostatic pressure effect to prevent the diffusion of the individual atoms. Thus, it can be concluded that the increase of the surface to volume ratio according to the decrease in the particle size results in the filler size-dependent variation of the elastic moduli of the nanocomposites.

However, there is no clear correlation between the grafting ratio and the normalized interaction energy. This result means that the fundamentals of the particle size effect originate from the geometrical feature consisting of the increased specific surface area of the nanoparticle and adsorption of the polymer molecules forming the interphase. This feature is also supported by the size dependent elastic stiffness of the 0% grafted nanocomposites. Even if the covalent grafting does not affect the particle size dependency in the nonbonding interaction energy itself, it is believed that the strong binding force through the covalent bond greatly increases the interfacial load transfer and affects the variation of the resultant elastic moduli according to the particle size. As the local hydrostatic pressure effect at the interphase is directly bridged to the anchoring effect afforded by the nanoparticle via the strong covalent bond, the reinforcing effect of the nanoparticle is dramatically magnified and, thus, the properties of the nanocomposites can be increased by up to 200% compared to that of the baseline properties of the nanocomposites estimated from the conventional continuum model(the Mori-Tanaka model prediction in Figure 2) and the particle size effect shows a long-range variation. This unusual behavior leaves a lot of suggestions in equivalent continuum modeling of nanocomposites with rigorous consideration of interfacial bonding condition to reproduce the particle size-dependent elastic moduli calculated from the MD simulations.

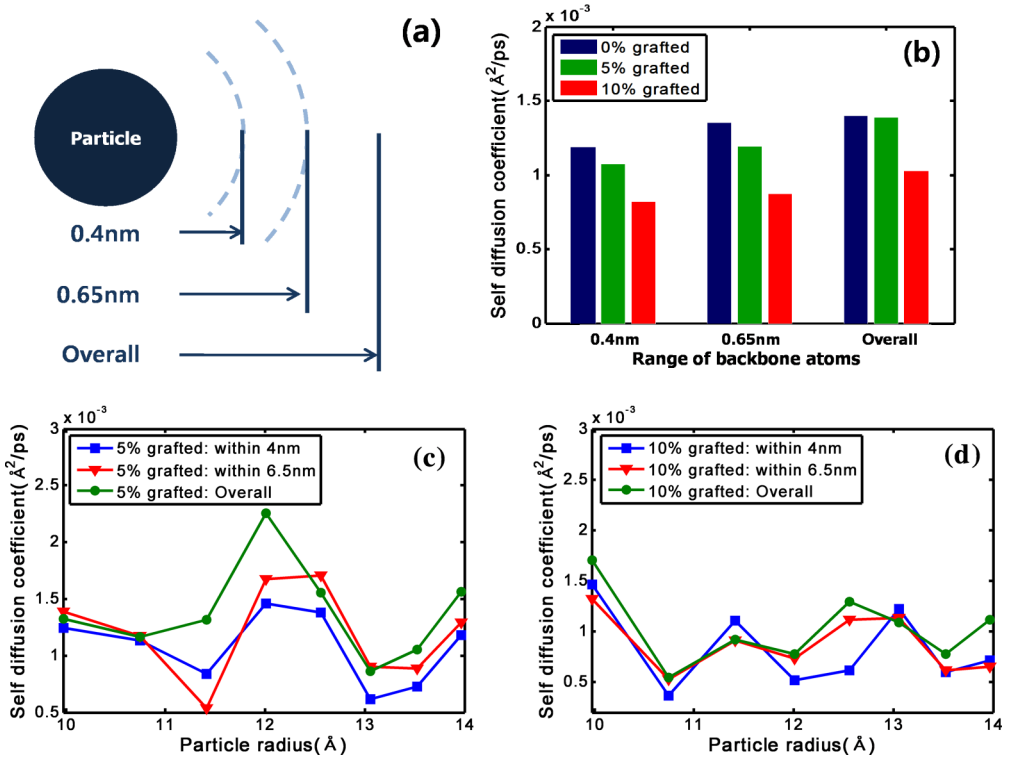

Figure 4. Self-diffusion coefficient of backbone atoms in the polyimide. (a) Definition of the range of backbone atoms in the polyimide, (b) Average self-diffusion coefficient over the whole particle radius according to the range of backbone atoms for the 0, 5, and 10% grafted nanocomposites. (c) Self-diffusion coefficient of matrix polymer in 5% grafted nanocomposite, and (d) 10% grafted nanocomposite according to the radius of the embedded nanoparticle.

dx.doi.org/10.1021/am301144z | ACS Appl. Mater. Interfaces 2012, 4, 4792–4799

Self-Diffusion Coefficient of Surrounding Matrix Polymer. The self-diffusion coefficients of the polyimide molecules are calculated from the mean squared displacement (MSD) of the nanocomposites, which is defined as[46,47]

$$\mathrm{MSD} = \left\langle \frac{1}{N}\sum_{i=1}^{N}(\mathbf{r}_i(t) - \mathbf{r}_i(0))^2 \right\rangle \tag{3}$$

where $\mathbf{r}_i$ is the position vector of the ith atom and N is the total number of atoms in the polyimide. As the MSD is a useful indicator to measure the average distance that the atoms in a system travel during finite time duration, it can be correlated with the self-diffusion coefficient as follows

$$D = \frac{1}{6}\lim_{t\to\infty}\frac{d}{dt}\left\langle \frac{1}{N}\sum_{i=1}^{N}(\mathbf{r}_i(t) - \mathbf{r}_i(0))^2 \right\rangle \tag{4}$$

During the 1.3 ns of the isothermal−isothermal ensemble simulation at 300 K and 1 atm to equilibrate the unit cells of the nanocomposites, we used the atomic trajectory saved during the last 300 ps of the simulations and used the least-squares fit of the MSD-simulation time curve to calculate the self-diffusion coefficient. In calculating its self-diffusion coefficient, we used only the trajectory of the backbone carbons in the polyimide because of their dominant role in the segmental motion and disentanglement. The range of the polyimide backbone for which the diffusion coefficient is calculated is divided into three regions according the radial distance from the surface of the nanoparticles, viz. 0.4 nm, 0.65 nm and the whole range of the polyimide zone, as shown in Figure 4a. The innermost zone within a radial distance of 0.4 nm is within the interphase zone where the density profile of the polyimide is quite different from that of the pure polyimide.[18] Thus, it can be intuitively inferred that the diffusivity of the polyimide in this region is lower than that in the other regions. In a recent molecular dynamics study on the effect of covalent grafting on the radial density distribution of the matrix polymer in nanocomposites, the density of such an interphase zone was found to decrease as the grafting ratio increases.[37] However, care must be taken to intuitively correlate the self-diffusion coefficient of the polyimide in grafted nanocomposites, because their covalent bonds act as a stronger anchor block to prevent the diffusion of the grafted polyimide than the densified interphase zone. Thus, not only the density of the interphase zone but also the covalent bonds at the interphase affect the self-diffusion of the polyimide matrix.

The self-diffusion coefficients of the polyimide molecules for each definition of the region in Figure 4a are depicted in Figure 4b. As the range of the backbone atoms increases, the diffusivity of the matrix polymer gradually increases. This indicates that the matrix molecules in the vicinity of the nanoparticle are more immobilized than those in the outermost regions, as reported in previous works.[48,49] This trend does explain the size effect of the nanocomposites. As the size of the nanoparticle decreases, the relative proportion of the innermost zone or interphase zone increases and, thus, more proportion of the polyimide molecules are strongly immobilized. For example, if the radius of the nanoparticle is small enough to have a very narrow region of polyimide whose radial distance is confined to a radial distance from the surface of the nanoparticle of less than 0.65 nm, the diffusion coefficient of the whole matrix molecule will be smaller than those of the larger nanoparticle embedded composites whose matrix region spans over a radial distance of 0.65 nm. In the equivalent continuum modeling of nanocomposites to characterize the particle size effect on the elastic moduli of nanocomposites,[19] a similar correlation between the relative volume fraction of the interphase zone and the resultant elastic stiffness of the nanocomposites has been revealed. As the grafting ratio increases, the self-diffusion coefficient of the polyimide backbones decreases, as expected.

However, as shown in panels c and d in Figure 4, there is no particle size dependency of the self-diffusion coefficient of the matrix polymer, even though the larger nanoparticle embedded nanocomposites have a greater number of grafted sites. This result is in contradiction with the results of a recent molecular dynamics simulation on the local diffusivity of grafted and ungrafted polystyrene in nanosilica reinforced composites by Ndoro et al.[50] According to their observations, the local diffusivity of the free chains in the ungrafted composites and that of those that penetrate into the grafted polymer brush in the grafted composites decrease as the size of the nanoparticle increases from 3 to 5 nm. To derive a more generalized conclusion on the local immobilization of the ungrafted chains and the filler size effect on this property, however, a study involving larger nanoparticles is required for the present molecular modeling. Moreover, there are some limitations to the application of the previous conclusion directly to the diffusion coefficient of the present nanocomposite molecular model. The molecular weight of the single polyimide chain considered in this study is much greater than the single polystyrene chain of 20 monomers considered in their simulation and one single polyimide chain in our model was allowed to have multiple grafted hydrocarbons, which is in discord with the previous modeling process that allowed only one grafting site per grafted polystyrene. Actually, the number of grafted sites per unit number of polyimide chains decreases as the radius of the nanoparticle decreases and, thus, the individual polyimide chain in the smaller nanoparticle-embedded cell naturally has a higher probability of having multiple grafting. Therefore, it is not appropriate for the present molecular model to distinguish the free and grafted chains and, consequently, we did not distinguish the diffusion coefficients of the grafted and ungrafted chains. As pointed out by Harton et al.,[51] even if the thickness of the interphase zone surrounding a small nanoparticle having a finite curvature is smaller than that at the flat surface of the identical material, which can reasonably represent an infinitely large particle, the resultant thermal diffusion of these interphases may not show any prominent difference. Likewise, even if the mobility of the adsorbed polymer in the nanocomposites is less confined by the smaller nanoparticles than larger ones, the relative contribution to the reinforcing effect should be correlated with the relative geometrical influence on the overall properties. Of particular importance in the reinforcing mechanism of the grafted nanoparticle with the filler size effect is the relative proportion of the immobilized interphase zone to the volume fraction of the other phases that constitute the microstructure of the nanocomposites.

To provide a better understanding of the conclusion concerning the contribution of the normalized nonbonding interaction between the nanoparticle and matrix, and the anchoring of the matrix molecule to prevent diffusion under mechanical loading through the covalent grafting to the embedded particle size dependent elastic moduli of the nanocomposites, we summarized the reinforcing mechanism in Figure 5. By varying the size of the embedded nanoparticles,

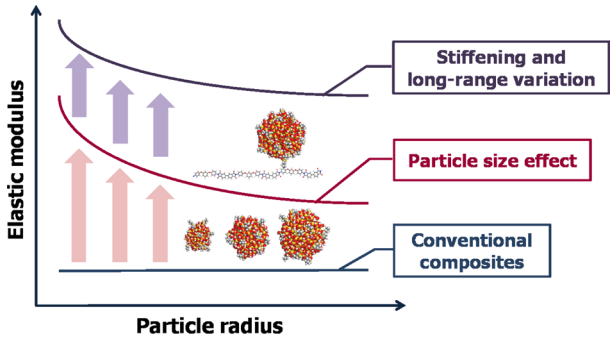

Figure 5. Schematic illustration of the reinforcing mechanism to distinguish the individual contribution of the embedded particle size and the interfacial covalent grafting to the filler size-dependent elastic moduli of the grafted polymer nanocomposites.

the resultant elastic moduli show a particle size effect as a result of the increased specific interfacial nonbonding interaction between the smaller nanoparticle and matrix. By covalently grafting the nanoparticles to the matrix polymer via a suitable synthesis to tailor the interfacial strength, the resultant elastic moduli of the nanocomposites can be stiffened again and the variation of the particle size-dependent elastic moduli according to the size of the nanoparticle shows a long-range variation.

SUMMARY AND CONCLUSIONS

Atomistic molecular dynamics simulations were utilized to identify the effect of the size of the embedded silica nanoparticles covalently grafted to the polyimide matrix on the overall elastic moduli of nanocomposites. Important findings obtained from the present MD simulations are as follows.

(1) At the fixed grafting ratio, the elastic moduli of nanocomposites increase as the radius of nanoparticle decreases.
(2) At each particle radius, the elastic moduli of nanocomposites increase as the covalent grafting ratio increases.
(3) The nonbonding interaction between the nanoparticle and matrix contribute to the filler size dependency in elastic stiffness.
(4) The covalent grafting only leads to the gradual and long-range variation of the size dependent elastic moduli and do not contribute to the size effect itself.

Although the present study dealt only with the linear elastic properties of composites by adopting nanoscale fillers, the nonlinear behavior of nanocomposites over a large strain range such as necking and drawing right after yielding can also be tailored by the size of the embedded nanoparticles and the grafted interface. Thus, more sophisticated approaches to these problems are still needed. Moreover, Even if we only concentrated on the filler size and grafting ratio of nanoparticulate composites, still there are other major factors that should be considered in computational modeling studies of nanocomposites such as the molecular weight of the matrix, types of filler and matrix, agglomeration of nanoparticles etc., which are still remaining as open issues in this field. Together with the MD simulations to account for those factors, establishing an efficient continuum modeling approaches to account for all of those factors is a very important issue to resolve inevitable computational inefficiency problem of MD simulations to design nanocomposites. On the basis of the present MD simulations, an efficient multiscale framework to account for the covalent grafting and the particle size effect will be proposed in the near future.

AUTHOR INFORMATION

Corresponding Author

*E-mail: mhcho@snu.ac.kr.

Notes

The authors declare no competing financial interest.

ACKNOWLEDGMENTS

This work was supported by the WCU (grant no. R31-2009-000-10083-0), funded by the MEST of the Korean government. Also, this work was supported by the National Research Foundation of Korea (NRF) grant funded by the Korea government (MEST) (No. 2012R1A3A2048841). The authors gratefully acknowledge this support.

REFERENCES

(1) Ajayan, P.; Stephan, O.; Colliex, C.; Trauth, D. *Science* **1994**, *265*, 1212−1214.
(2) Thostenson, E.; Li, C.; Chou, T.-W. *Compos. Sci. Technol.* **2005**, *65*, 491−516.
(3) Liff, S.; Kumar, N.; McKinley, G. *Nat. Mater.* **2007**, *6*, 76−83.
(4) Finningan, B.; Jack, K.; Campbell, K.; Halley, P.; Truss, R.; Casey, P.; Cookson, D.; King, S.; Martin, D. *Macromolecules* **2005**, *38*, 7386−7396.
(5) Mahfuz, H.; Hasan, M.; Dhanak, V.; Beamson, G.; Stewart, J.; Rangari, V.; Wei, X.; Khabashesku, V.; Jeelani, S. *Nanotechnology* **2008**, *19*, 445702.
(6) Brown, D.; Marcadon, V.; Mélé, P.; Albérola, N. *Macromolecules* **2008**, *41*, 1499−1511.
(7) Cho, J.; Joshi, M.; Sun, C. *Compos. Sci. Technol.* **2006**, *66*, 1941−1952.
(8) Chisholm, N.; Mahfuz, H.; Rangari, V.; Ashfaq, A.; Jeelani, S. *Compos. Struct.* **2005**, *67*, 115−124.
(9) Mishira, S.; Sonawane, S.; Singh, R. *J. Polym. Sci., Polym. Phys.* **2005**, *43*, 107−113.
(10) Ng, C.; Ash, B.; Schadler, L.; Siegel, R. *Adv. Compos. Lett.* **2001**, *10*, 101−111.
(11) Douce, J.; Boilot, J.-P.; Biteau, J.; Scodellaro, L.; Jimenez, A. *Thin Solid Films* **2004**, *466*, 114−122.
(12) Goyal, R.; Tiwari, A.; Mulik, U.; Negi, Y. *J. Phys. D: Appl. Phys.* **2008**, *41*, 085403.
(13) Goertzen, W.; Kessler, M. *J. Appl. Polym. Sci.* **2008**, *109*, 647−653.
(14) Prathab, B.; Aminabhavi, T.; Parthasarathi, R.; Manikandan, P.; Subramanian, V. *Polymer* **2006**, *47*, 6914−6924.
(15) Prathab, B.; Aminabhavi, T. *Langmuir* **2007**, *23*, 5439−5444.
(16) Prathab, B.; Subramanian, V.; Aminabhavi, T. *Polymer* **2007**, *48*, 409−416.
(17) Adnan, A.; Sun, C.; Mahfuz, H. *Compos. Sci. Technol.* **2007**, *67*, 348−356.
(18) Yang, S.; Cho, M. *Appl. Phys. Lett.* **2008**, *93*, 043111.
(19) Yang, S.; Cho, M. *Appl. Phys. Lett.* **2009**, *94*, 223104.
(20) Yu, S.; Yang, S.; Cho, M. *Polymer* **2009**, *50*, 945−952.
(21) Liu, J.; Wu, S.; Zhang, L.; Wang, W.; Cao, D. *Phys. Chem. Chem. Phys.* **2011**, *13*, 518−529.
(22) Cho, J.; Sun, C. *Comput. Mater. Sci.* **2007**, *41*, 54−62.
(23) Papakonstantopoulos, G.; Yoshimoto, K.; Doxastakis, M.; Nealey, P.; de Pablo, J. *Phys. Rev. E* **2005**, *72*, 031801.
(24) Yang, S.; Yu, S.; Cho, M. *J. Appl. Phys.* **2010**, *108*, 056102.
(25) Choi, J.; Yu, S.; Yang, S.; Cho, M. *Polymer* **2011**, *52*, 5197−5203.
(26) Vollenberg, P.; de Haan, J.; van de Ven, L.; Heikens, D. *Polymer* **1989**, *30*, 1663−1668.

(27) Cipari, D.; Jacob, K.; Tannenbaum, R. *Macromolecules* **2006**, *39*, 6565−6573.
(28) Maiti, M.; Bhowmick, A. *Polymer* **2006**, *47*, 6156−6166.
(29) Chen, K.; Zheng, L.; Tian, X.; Hu, K.; Wang, R.; Liu, C.; Li, Y.; Cui, P. *Macromolecules* **2010**, *43*, 1076−1082.
(30) Sun, Y.; Zhang, Z.; Wong, C. *J. Colloid Interface Sci.* **2005**, *292*, 436−444.
(31) Kim, Y.-J.; Ha, S.-W.; Jeon, S.-M.; Yoo, D.; Chun, S.-H.; Sohn, B.-H.; Lee, J.-K. *Langmuir* **2010**, *26*, 7555−7560.
(32) Gojny, F.; Nastalczyk, J.; Roslaniec, Z.; Schulte, K. *Chem. Phys. Lett.* **2003**, *370*, 820−824.
(33) Chevigny, C.; Dalmas, F.; Cola, E.; Gigmes, D.; Bertin, D.; Boué, F.; Jestin, J. *Macromolecules* **2011**, *44*, 122−133.
(34) Guo, Z.; Pereira, T.; Choi, O.; Wang, Y.; Hahn, H. *J. Mater. Chem.* **2006**, *16*, 2800−2808.
(35) Cheng, H.; Sahoo, N.; Tan, Y.; Pan, Y.; Bao, H.; Li, L.; Chan, S.; Zhao, J. *ACS Appl. Mater. Interfaces* **2012**, *4*, 2387−2394.
(36) Roy, A.; Farmer, B.; Varshney, V.; Sihn, S.; Lee, J.; Ganguli, S. *ACS Appl. Mater. Interfaces* **2012**, *4*, 545−563.
(37) Ndoro, T.; Voyiatzis, E.; Ghanbari, A.; Theodorou, D.; Böhm, M.; Müller-Plathe, F. *Macromolecules* **2011**, *44*, 2316−2327.
(38) *Material Studio 5.0*; Accelrys Inc.: San Diego, CA.
(39) Odegard, G.; Clancy, T.; Gates, T. *Polymer* **2005**, *46*, 553−562.
(40) Tsai, J.-L.; Tzeng, S.-H. *J. Compos. Mater.* **2008**, *42*, 2345−2361.
(41) Andersen, H. *J. Chem. Phys.* **1980**, *72*, 2384−2393.
(42) Varshney, V.; Patnaik, S. S.; Roy, A.; Farmer, B. *Macromolecules* **2008**, *41*, 6837−6842.
(43) Berendsen, H.; Postma, J.; van Gunsteren, W.; DiNola, A.; Haak, J. *J. Chem. Phys.* **1984**, *81*, 3684−3690.
(44) Parrinello, M.; Rahman, A. *Phys. Rev. Lett.* **1980**, *45*, 1196−1199.
(45) Parrinello, M.; Rahman, A. *J. Chem. Phys.* **1982**, *76*, 2662−2666.
(46) Prathab, B.; Aminabhavi, T. *J. Polym. Sci., Polym. Phys.* **2007**, *45*, 1260−1270.
(47) Jawalkar, S.; Aminabhavi, T. *Polym. Int.* **2007**, *56*, 928−934.
(48) Liu, J.; Wu, Y.; Shen, J.; Gao, Y.; Zhang, L.; Cao, D. *Phys. Chem. Chem. Phys.* **2011**, *13*, 13058−13069.
(49) Kropka, J.; Putz, K.; Pryamitsyn, V.; Ganesan, V.; Green, P. *Macromolecules* **2007**, *40*, 5424−5432.
(50) Ndoro, T.; Böhm, M.; Müller-Plathe, F. *Macromolecules* **2012**, *45*, 171−179.
(51) Harton, S.; Kumar, S.; Yang, H.; Koga, T.; Hicks, K.; Lee, H.; Mijovic, J.; Liu, M.; Vallery, R.; Gidley, D. *Macromolecules* **2010**, *43*, 3415−3421.